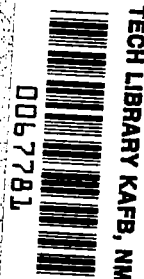


**NASA
Technical
Paper
2008**

April 1982

NASA
TP
2008
c.1



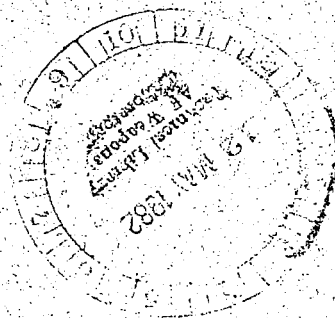
Three-Dimensional Relativistic Field-Electron Interaction in a Multicavity High-Power Klystron

II - Working Equations

Henry G. Kosmahl

AFWL/SUL
TECHNICAL LIBRARY
KIRTLAND AFB, NM 87117

NASA





Three-Dimensional Relativistic Field-Electron Interaction in a Multicavity High-Power Klystron

II - Working Equations

Henry G. Kosmahl
*Lewis Research Center
Cleveland, Ohio*



National Aeronautics
and Space Administration

Scientific and Technical
Information Branch

SUMMARY

A computation package containing all equations and procedures needed in designing a high-power multicavity klystron amplifier has been developed. The rigorously derived three-dimensional relativistic axisymmetric equations of motion are used to compute the bunched current and the induced RF gap voltage for all interaction cavities except the input and second cavities, where the linear space-charge wave theory data are employed in order to reduce the computation time. Both distance-step and time-step integration methods are used to compute the Fourier coefficients of both the beam current and induced current.

INTRODUCTION

This report describes in detail a design computation package of a magnetically focused high-power multicavity klystron amplifier. The theoretical foundation is based on the investigation of field-electron interactions of a relativistic klystron described in a previous report (ref. 1). The computation method is based on the large-signal disk-electron model which can be programmed and run on a large-capacity high-speed computer. The unmodulated electron beam which enters the input cavity is divided into a large number of deformable disks of electrons, and each disk is subdivided into an equal number of rings of electrons which serve as elementary charges in the mathematical model. Thirty-two disks per one space-charge wavelength and three rings per disk were used in the computation model. Each of the ninety-six rings is followed through from the input cavity gap, to the intermediate interaction gaps, and to the drift-tube spaces until the output gap is reached. The induced current and the RF gap voltage of the various cavities are computed on the basis of the theory of Shockley and Ramo. The fundamental bunched current and the induced RF gap voltage of the various cavities are computed, first, by performing the distance-step integration of the equations of motion to yield the precise data of the position and phase of the individual rings and second, by evaluating the Fourier coefficients of the bunched beam current and the induced RF gap voltage by using the time-step integration method. Beam loading and cavity detuning effects are appropriately dealt with. Space-charge force Green functions, G_E and G_0 , are modified to take into consideration relativistic velocity of the beam motion. Since the RF gap voltage and the beam loading parameters, $G_{b,s}$ and $B_{b,s}$, are interrelated, an iteration process is employed to determine the voltage modulation index for the various gaps. However, in order to reduce the computation time the linear space-charge wave theory data were used to design the input and second cavities, where small voltage modulation index values will be used.

Material, not previously published, presented at the International Electron Devices Meeting sponsored by the Institute of Electrical and Electronic Engineers, Washington, D.C., October 11, 1971, and the Solar Power Space System Workshop sponsored by NASA Lyndon B. Johnson Space Center, Houston, Texas, January 15-18, 1979.

This report consists of three main parts:

- (1) All input data and initial computation formulas needed to start the computer program
- (2) All working equations used in various stages of computation
- (3) Design procedures described in detail, including the method of iteration in the computation of the voltage modulation index of the various gaps

In addition, four appendixes are included at the end of this report so that the origin of some of these working equations can be traced and checked.

INPUT DATA

Design Parameters

The following are the parameters and data to be specified by the designer:

- (1) Klystron operational frequency, f_0 , in hertz. (This is also the input drive frequency of the klystron.)
- (2) Input drive power, P_{in} , in watts. (Matched condition is assumed.)
- (3) Direct-current beam current, I_0 , in amperes, which is related to the relativistic perveance K_r by the equation

$$K_r = K_0 \left(1 - \frac{3}{28} \frac{V_0}{V_{eq}} \right)$$

where $K_0 = I_0/(V_0)^{3/2}$ is the nonrelativistic perveance, and $V_{eq} = m_0 c^2 / |e| = 5.11 \times 10^5$ volts is the equivalent beam voltage.

- (4) Direct-current beam voltage, V_0 , in volts.
- (5) External applied dc magnetic field as measured along the z-axis, B_0 , in weber per meter squared. ($1 \text{ Wb/m}^2 = 10\,000 \text{ G}$).
- (6) Tunnel diameter, $2a$, in meters.
- (7) Direct-current beam diameter at the entrance to the input cavity, $2b$, in meters.
- (8) Diameter of the cathode, $2r_c$, in meters.
- (9) Physical gap length of the s^{th} cavity, $2\ell_s$, in meters, with $s = 1, 2, \dots$; that is, for a five-cavity klystron, $2\ell_1, 2\ell_2, 2\ell_3, 2\ell_4$, and $2\ell_5$.
- (10) Drift-tube length, L_s , in meters, as measured between the centers of the s^{th} and the $(s \pm 1)^{\text{th}}$ cavities; that is, L_1, L_2, L_3, L_4 , and L_5 . It is to be noted that the drift-tube length may be determined initially by the small-signal space-charge wave theory data given by

$$L_s = \frac{\lambda_{sp,s}(s)}{4} = (2m + 1) \frac{\pi}{2} \frac{u_0}{\omega_{p0}}$$

where $m = 0, 1, \dots$ and

- λ_e electronic wavelength, $\frac{u_0}{f}$
- λ_{sp} space-charge wavelength
- u_0 relativistic dc beam velocity, $5.93 \times 10^5 R_u \sqrt{V_0}$, m/sec
- ω_{p0} plasma radian frequency, $\sqrt{\frac{|e/m_0|}{\epsilon_0}} \sqrt{\frac{I_0}{\pi b^2 u_{00}}}$

R_u relativistic velocity reduction factor,

$$\sqrt{1 + \frac{V_0}{2 V_{eq}}} / \left(1 + \frac{V_0}{V_{eq}}\right)$$

u_{00} nonrelativistic dc beam velocity, $5.93 \times 10^5 \sqrt{V_0}$, m/sec

- (11) $\omega_0 = 2\pi f_0 / u_0$.
- (12) $k = 2\pi f_0 / c$.
- (13) Nonrelativistic cyclotron radian frequency, $\omega_{c0} = (e/m_0)B_0$
- (14) Unloaded Q of the s^{th} cavity, $Q_{u,s}$; that is, $Q_{u,1}$, $Q_{u,2}$, $Q_{u,3}$, $Q_{u,4}$, and $Q_{u,5}$.
- (15) External Q of the s^{th} cavity, $Q_{ext,s}$; that is, $Q_{ext,1}$ and $Q_{ext,5}$ ($Q_{ext,2}$, $Q_{ext,3}$, and $Q_{ext,4} = \infty$).
- (16) Characteristic impedance of the s^{th} cavity, $(R/Q)_s$; that is, $(R/Q)_1$, $(R/Q)_2$, $(R/Q)_3$, $(R/Q)_4$, and $(R/Q)_5$.
- (17) Frequency-tuning parameter of the s^{th} cavity $\delta_{u,s} = (f_{tuned} \pm f_{resonant}) / f_{resonant}$; that is, $\delta_{u,2}$, $\delta_{u,3}$, and $\delta_{u,4}$ ($\delta_{u,1}$ and $\delta_{u,5} = 0$).
- (18) Field-shape parameter of the s^{th} cavity, H_s ; that is, H_1 , H_2 , H_3 , H_4 , and H_5 .
- (19) Number of disks in one space-charge wavelength used in the design model (here 32), N, and number of rings in each disk (here 3), R.

Physical Constants Used in Computation

The following physical constants (expressed in SI units) are needed in the computation:

- (1) Velocity of light, $c = 3 \times 10^8$ m/sec
- (2) Dielectric permittivity of the vacuum, $\epsilon_0 = (1/36 \pi) \times 10^{-9} = 8.854 \times 10^{-12}$ F/m
- (3) Magnetic permeability of the vacuum, $\mu_0 = 4\pi \times 10^{-7}$ H/m
- (4) Rest mass of the electron, $m_0 = 9.108 \times 10^{-31}$ kg
- (5) Magnitude of the electronic charge, $|e| = 1.602 \times 10^{-19}$ C
- (6) Ratio of electron charge to rest mass, $|e/m_0| = 1.759 \times 10^{11}$ C kg⁻¹
- (7) Equivalent beam voltage, $V_{eq} = m_0 c^2 / |e| = 5.11 \times 10^5$ V

WORKING EQUATIONS

Normalized Equations of Motion

The normalized axial equation of motion is

$$\ddot{\xi}_s = \frac{\alpha_s \cos \theta_s P_0 \frac{H_s \ell}{\sinh[H_s a(\ell_s/a)]}}{4 \frac{\ell_s}{a} (\beta_e a)^2} \left\{ (ka)^2 \ddot{\xi}_\rho \begin{pmatrix} G_\rho \\ F_\rho \end{pmatrix} + [(ka)^2 \dot{\xi}^2 - 1] \begin{pmatrix} G_\xi \\ F_\xi \end{pmatrix} \right\} \\ + \frac{\pi}{NR} \left(\frac{\omega_{p0}}{\omega} \right)^2 \frac{P_0}{\beta_e a} [1 - (ka)^2 \dot{\xi}^2] \mathcal{G}'_\xi + \frac{P_0^2}{2\rho} \left(\frac{\omega_{c0}}{\omega} \right)^2 \frac{B_r}{B_0} \frac{\psi - \left(\frac{r_i}{r_e} \right)^2 \psi_c}{\psi_a} \quad (1)$$

The normalized radial equation of motion is

$$\ddot{\rho}_s = \frac{\alpha_s \cos \theta_s P_0 \frac{H_s \ell}{\sinh[H_s a(\ell_s/a)]}}{4 \frac{\ell_s}{a} (\beta_e a)^2} \left\{ [1 - (ka)^2 \dot{\rho}^2] \begin{pmatrix} G_\rho \\ F_\rho \end{pmatrix} - (ka)^2 \dot{\rho} \dot{\xi} \begin{pmatrix} G_\xi \\ F_\xi \end{pmatrix} \right\} \\ + \frac{\pi}{NR} \left(\frac{\omega_{p0}}{\omega} \right)^2 \frac{P_0}{\beta_e a} \left\{ [1 - (ka)^2 (\dot{\rho}^2 + \dot{\xi}^2)] \mathcal{G}'_\rho - (ka)^2 \dot{\rho} \dot{\xi} \mathcal{G}'_\xi \right\} \\ + \frac{P_0^2}{4\rho^3} \left(\frac{\omega_{c0}}{\omega} \right)^2 \left\{ \left[\frac{\psi - \left(\frac{r_i}{r_e} \right)^2 \psi_c}{\psi_a} \right]^2 - 2\rho^2 \frac{B_z}{B_0} \frac{\psi - \left(\frac{r_i}{r_e} \right)^2 \psi_c}{\psi_a} \right\} \quad (2)$$

The independent variables are ξ , $\rho_{0,eq,j}$, and $\phi_{0,j}$, defined as

ξ normalized axial coordinate, z/a

$\rho_{0,eq,j}$ normalized equivalent charge center of j^{th} ring charge element at entrance to input cavity

$\phi_{0,j}$ entry phase of j^{th} disk charge element where $j = 1, 2, \dots, 32 (=NR)$ in a 32-disk 3-ring model, $2\pi j/N$

The independent variables are ρ , ϕ , $\dot{\rho}$, and $\dot{\xi}$, defined as

ρ normalized radial coordinate, r/a

$\dot{\rho}(\xi, \rho_0, eq, j, \phi_{0,j})$ normalized radial velocity component of j^{th} ring charge element, where $\theta = \omega t$, $d\rho/d\theta$

$\dot{\xi}(\xi, \rho_0, eq, j, \phi_{0,j})$ normalized axial velocity component of j^{th} ring charge element, $d\xi/d\theta = z/\omega a$

$\phi(\xi, \rho_0, eq, j, \phi_{0,j})$ phase variable which defines phase position of j^{th} ring charge element relative to RF gap field as a function of displacement and initial state of entering electron beam, $\theta - (\beta_{ea})\xi$

The following are the relationships or equations needed to compute equations (1) and (2):

(1) Relativity parameter:

$$p_0 = \sqrt{\frac{1 - (ka)^2 (\dot{\rho}^2 + \dot{\xi}^2)}{1 + 0.25 (ka)^2 \left(\frac{\omega c_0}{\omega}\right)^2 \left(\frac{\psi - \psi_c}{\psi_a}\right)^2}}$$

where

$$\psi = 2\pi \int_0^{\rho} B_{\xi}(\rho, \xi) \rho \, d\rho$$

ψ_a tunnel flux, $\pi a^2 B_0$

ψ_c cathode flux, $\pi r_c^2 B_0$

r_c cathode radius

$B_{\rho}(\rho, \xi)$, $B_{\xi}(\rho, \xi)$ radial and axial components of dc magnetic fields given by eqs. (3) and (4) in the section Calculation of External Direct-Current Magnetic Fields B_{ρ} and B_{ξ}

(2) Four field-shape functions, F_ξ , F_ρ , G_ξ , and G_ρ :

$$F_\xi(\xi, \rho) = \cosh(H_s a \xi) \frac{J_0 \left[\rho \sqrt{(ka)^2 + (H_s a)^2} \right]}{J_0 \left[\sqrt{(ka)^2 + (H_s a)^2} \right]} - \sum_{n=1}^{\infty} \frac{\lambda_n J_0(\lambda_n \rho)}{p_n J_1(\lambda_n)} \left(\frac{e^{H_s a \xi / a}}{p_n - H_s a} + \frac{e^{-H_s a \xi / a}}{p_n + H_s a} \right) e^{-p_n \xi / a} \cosh(p_n |\xi|)$$

for $-\xi_s / a \leq \xi \leq \xi_s / a$

$$F_\rho(\xi, \rho) = -H_s \sinh(H_s a \xi) \frac{J_1 \left[\rho \sqrt{(ka)^2 + (H_s a)^2} \right]}{\sqrt{k^2 + H_s^2} J_0 \left[\sqrt{(ka)^2 + (H_s a)^2} \right]} + \sum_{n=1}^{\infty} \frac{J_1(\rho \lambda_n)}{J_1(\lambda_n)} \left(\frac{e^{H_s a \xi / a}}{p_n - H_s a} + \frac{e^{-H_s a \xi / a}}{p_n + H_s a} \right) e^{-p_n \xi / a} \sinh(p_n |\xi|)$$

for $-\xi_s / a \leq \xi \leq \xi_s / a$

$$G_\xi(\xi, \rho) = \sum_{n=1}^{\infty} \frac{\lambda_n J_0(\rho \lambda_n)}{p_n J_1(\lambda_n)} \left[\frac{\sinh(p_n + H_s a) \frac{\xi_s}{a}}{p_n + (H_s a)} + \frac{\sinh(p_n - H_s a) \frac{\xi_s}{a}}{p_n - (H_s a)} \right] e^{-p_n |\xi|} \quad \text{for } |\xi| > \frac{\xi_s}{a}$$

$$G_{\rho}(\xi, \rho) = \sum_{n=1}^{\infty} \frac{J_1(\rho \lambda_n)}{J_1(\lambda_n)} \left[\frac{\sinh(p_n + H_s a) \frac{\ell_s}{a}}{p_n + (H_s a)} + \frac{\sinh(p_n - H_s a) \frac{\ell_s}{a}}{p_n - (H_s a)} \right] e^{-p_n |\xi|} \text{ for } |\xi| > \frac{\ell_s}{a}$$

(3) Two Green function space-charge forces, \mathcal{G}'_{ξ} and \mathcal{G}'_{ρ} :

$$\mathcal{G}'_{\xi}(\xi, \rho) = \sum_{n=1}^{\infty} \sum_{\text{all } \xi_0, \rho_0} \frac{J_0(\rho \lambda_n) J_0(\rho_0 \lambda_n)}{J_1^2(\lambda_n)} e^{-\frac{\lambda_n |\xi - \xi_0| R}{\sqrt{1 - (u_{01}/c)^2}}} \text{sign} \frac{\xi - \xi_0}{\sqrt{1 - \left(\frac{u_0}{c}\right)^2}}$$

$$\mathcal{G}'_{\rho}(\xi, \rho) = \sqrt{1 - \left(\frac{u_{00}}{c}\right)^2} \sum_{n=1}^{\infty} \sum_{\text{all } \xi_0, \rho_0} \frac{J_1(\rho \lambda_n) J_0(\rho_0 \lambda_n)}{J_1^2(\lambda_n)} e^{-\frac{\lambda_n |\xi - \xi_0| R}{\sqrt{1 - (u_{01}/c)^2}}}$$

where J_0 and J_1 are Bessel functions of the first kind, λ_n is the n^{th} root of the Bessel function,

$$\text{sign } \xi - \xi_0 = \begin{cases} 1 & \text{for } \xi > \xi_0 \\ -1 & \text{for } \xi < \xi_0 \end{cases}$$

$$p_n = \sqrt{\lambda_n^2 - (ka)^2}$$

The notation $(\xi - \xi_0)_R$ implies that the value inside the parentheses must be computed by using the retarded positions defined by

$$d = \sqrt{(z_b - z_a)^2 + (r_{eq,b} - r_{eq,a})^2}$$

or

$$(d/a) = \sqrt{(\xi_b - \xi_a)^2 + (\rho_{eq,b} - \rho_{eq,a})^2}$$

(see fig. 1); that is, if we wish to calculate the force acting on the charge located at ξ at time t (i.e., θ) due to a charge at ξ_0 , we must take the value of charge at time $t - |z - z_0|/c$, or more precisely, $t - d/c$, where d is given above and c is the velocity of light.

Calculation of External Direct-Current Magnetic Fields B_0 and B_x

With reference to figure 2, we note that the radial and axial components of the external dc magnetic field produced by an electromagnet are given by (appendix A)

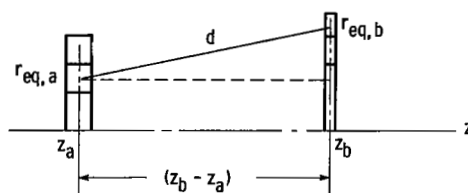


Figure 1. - Computation of space charge forces between disks (rings).

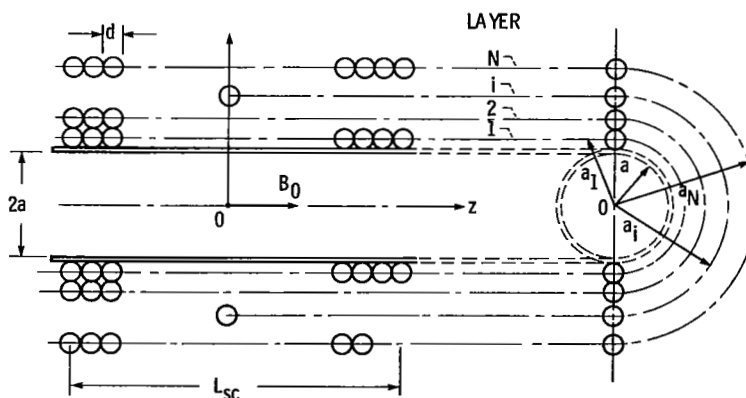


Figure 2. - Configuration of close-wound N-layer solenoid.

$$B_{\rho}(\xi, \rho) = B_0 \sum_{n=1}^N \frac{\int_0^{\infty} K_1(ka_i) I_1(k\rho) \sin(ka\xi) \sin \frac{L_{sc}}{2a} ka dk}{\int_0^{\infty} K_1(ka_i) \sin \frac{L_{sc}}{2a} ka dk} \quad (3)$$

$$B_{\xi}(\xi, \rho) = B_0 \sum_{n=1}^N \frac{\int_0^{\infty} K_1(ka_i) I_0(k\rho) \sin(ka\xi) \sin \frac{L_{sc}}{2a} ka dk}{\int_0^{\infty} K_1(ka_i) \sin \frac{L_{sc}}{2a} ka dk} \quad (4)$$

where I_0 , I_1 , and K_1 are modified Bessel functions of the first kind; B_0 is the magnetic field along the z-axis; and a_i is the mean radius of the i^{th} layer. It has the following simple relation with the diameter d of the wire used:

$$a_i = a_1 + (i - 1)d$$

where a_1 is the mean radius of the first layer of the solenoid.

Calculation of Fundamental Bunched Current for Third and Succeeding Cavities, $s = 3, 4, \dots$, Including Output Cavity

The fundamental beam current when normalized to the dc beam current I_0 is given by (appendix B)

$$\frac{I_{b,s}}{I_0} = \sqrt{\bar{A}_s^2 + \bar{B}_s^2} e^{-j\Delta_{b,s}} \quad (5)$$

where

$$\bar{A}_s = \frac{-2}{NR} \sum_{j=1}^{NR=96} \delta_{\xi, \xi_s} \cos \phi_j(\rho_0, eq, \phi_0; \xi_s) \quad (6)$$

$$\bar{B}_s = \frac{-2}{NR} \sum_{j=1}^{NR=96} \delta_{\xi, \xi_s} \sin \phi_j(\rho_0, eq, \phi_0; \xi_s) \quad (7)$$

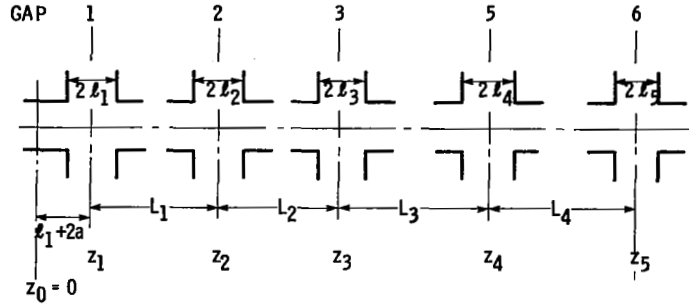


Figure 3. - Identification of various interaction gaps and drift-tube spaces in five-cavity klystron.

$$\Delta_{b,s} = \arctan \frac{\overline{B}_s}{\overline{A}_s} \quad (8)$$

where the bar over the symbols A_s and B_s indicates they are normalized Fourier coefficients, and

$$\delta_{\xi, \xi_s} = \begin{cases} 1 & \text{for } \xi = \xi_s \text{ (i.e., } z = z_s) \\ 0 & \text{for } \xi \neq \xi_s \text{ (i.e., } z \neq z_s) \end{cases}$$

in which ξ_s (i.e., z_s) is referred to the midplane of the s th cavity gap (fig. 3) with

$$\xi_s = \frac{z_s}{a} = \left(\frac{l_1}{a} + 2 \right) + \sum_{i=1}^s \frac{L_{i-1}}{a} \quad \text{for } i = 1, 2, 3, \dots \quad (9)$$

For example, for the fifth cavity, $s = 5$ (see fig. 3),

$$\xi_5 = \left(\frac{l_1}{a} + 2 \right) + \frac{L_1}{a} + \frac{L_2}{a} + \frac{L_3}{a} + \frac{L_4}{a}$$

The equivalent charge center $\rho_{0,eq,j}$ (i.e., $r_{0,eq,j}$) of the j th ring charge element is determined by the design data shown in figures 4 and 5

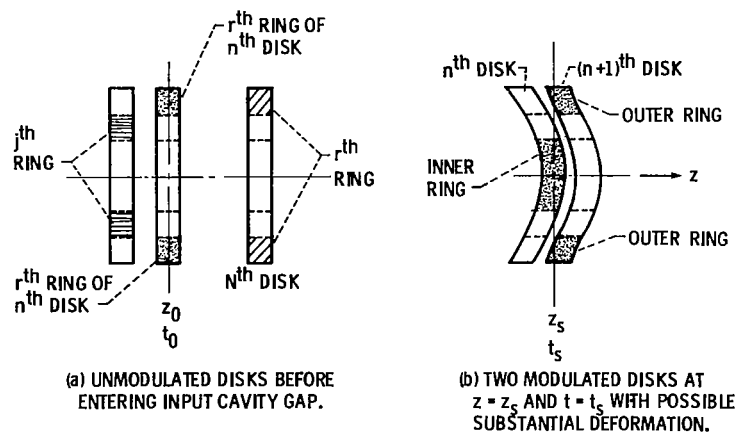


Figure 4. - Unmodulated and modulated beam disks.

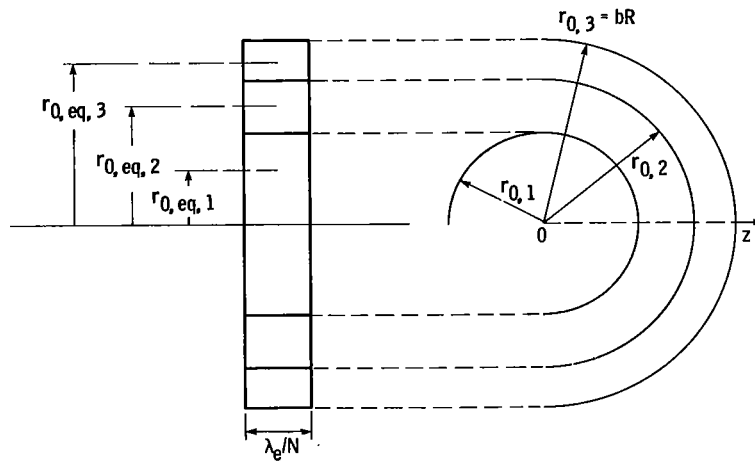


Figure 5. - Computation of charge center.

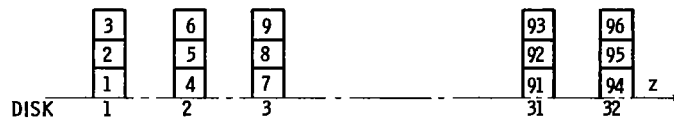


Figure 6. - Identification of ring charge element of three-ring 32-disk model.

$$\left. \begin{aligned} \rho_{0,eq,1} &= \frac{r_{0,eq,1}}{a} = \frac{b}{a} \frac{R}{\sqrt{6}} \\ \rho_{0,eq,2} &= \frac{r_{0,eq,2}}{a} = \frac{b}{a} \frac{R}{\sqrt{2}} \\ \rho_{0,eq,3} &= \frac{r_{0,eq,3}}{a} = \frac{b}{a} \frac{R}{\sqrt{\frac{5}{6}}} \end{aligned} \right\} \quad (10)$$

In order to facilitate the computation, we introduce the equivalent charge center with the general index j and the index r to designate the ring of a given disk. Then, for a three-ring model ($R = 3$), $r = 1, 2$, and 3 . Furthermore, if we introduce a second index d to designate the number of disks under consideration, with $d = 1, 2, \dots, 32$ for a 32-disk model, we can replace the index j in $\rho_{0,eq,j}$ by

$$j = 3(d - 1) + r$$

for

$$r = 1, 2, \text{ and } 3(R)$$

$$d = 1, 2, \dots, 32(N)$$

For example, with reference to figure 6, we note that the 95th ring charge element ($j = 95$) is identified as the second ring ($r = 2$) of the 32nd disk ($d = 32$); hence

$$j = 3(32 - 1) + 2 = 95$$

On the other hand, since each disk and each ring become distorted and deformed after the beam has passed through the input modulation gap, in order to identify and follow the movement of a given ring charge element the following equation is used instead:

$$r_{s,eq,j} = r_{0,eq,j} + \int_0^t \frac{dr}{dt} dt$$

or

$$\rho_{s,eq,j} = \frac{r_{s,eq,j}}{a} = \rho_{0,eq,j} + \int_0^\theta \dot{a} \rho d\theta \quad (11)$$

Calculation of Beam Parameters $G_{b,s}$ and $B_{b,s}$

The beam conductance $G_{b,s}$ and the beam susceptance $B_{b,s}$ needed to compute the gap voltage modulation index α_s are determined by (appendix B)

$$G_{b,s} = \frac{G_0}{\alpha_s} \sqrt{\bar{A}_s^2 + \bar{B}_s^2} \cos x_s \quad (12)$$

$$B_{b,s} = \frac{G_0}{\alpha_s} \sqrt{\bar{A}_s^2 + \bar{B}_s^2} \sin x_s \quad (13)$$

where

$$G_0 = \frac{I_0}{V_0}$$

$$x_s = \arctan(2Q_{T,s} \delta_{T,s}) + \arctan \frac{\bar{D}_s}{\bar{C}_s} - \arctan \frac{\bar{B}_s}{\bar{A}_s} \quad (14)$$

with \bar{A}_s and \bar{B}_s given by equations (6) and (7), \bar{C}_s and \bar{D}_s given by equations (16) in the next section, and α_s given by equations (18) in the section following that.

Calculation of Induced Current $I_{i,s}$

The normalized fundamental induced current is given by (appendix C)

$$\frac{I_{i,s}}{I_0} = \sqrt{\bar{C}_s^2 + \bar{D}_s^2} e^{-j\Delta_{i,s}} \quad (15)$$

where \bar{C}_s and \bar{D}_s are the normalized Fourier coefficients given by

$$\begin{pmatrix} \bar{C}_s \\ \bar{D}_s \end{pmatrix} = \frac{-2\pi Ha}{MNR \sinh\left(Ha \frac{s_s}{a}\right)} \sum_{m=1}^{M=36} \sum_{\text{all } k} \delta_{\xi, \xi_k} \sum_{j=1}^{NR=96} \left[\begin{matrix} \cdot \\ \rho_j \end{matrix} \begin{pmatrix} F_\rho \\ G_\rho \end{pmatrix} + \begin{matrix} \cdot \\ \xi_j \end{matrix} \begin{pmatrix} F_\xi \\ G_\xi \end{pmatrix} \right] \begin{pmatrix} \cos \phi_m(\rho_{0,eq,j}, \phi_0; \rho_{eq,j}, \xi_k, \phi_s) \\ \sin \phi_m(\rho_{0,eq,j}, \phi_0; \rho_{eq,j}, \xi_k, \phi_s) \end{pmatrix} \quad (16)$$

and

$$\Delta_{i,s} = \arctan \frac{\overline{D}_s}{\overline{C}_s} \quad (17)$$

with

$$\delta_{\xi, \xi_k} = \begin{cases} 1 & \text{for } \xi = \xi_k \\ 0 & \text{for } \xi \neq \xi_k \end{cases}$$

$$\xi_s - \left(\frac{\lambda_s}{a} + 2 \right) \leq \xi_k \leq \xi_s + \left(\frac{\lambda_s}{a} + 2 \right)$$

It is to be noted that (1) the two equivalent charge centers $\rho_{0,eq,j}$ and $\rho_{k,eq,j}$ are determined in accordance with rules detailed in the section Calculation of Fundamental Bunched Current for Third and Succeeding Cavities, $s = 3, 4, \dots$, Including Output Cavity and (2) the two normalized velocity components $\dot{\rho}_j$ and $\dot{\xi}_j$ are to be computed as functions of

$$\begin{pmatrix} \dot{\rho}_j \\ \dot{\xi}_j \end{pmatrix} = \begin{pmatrix} \dot{\rho}_j \\ \dot{\xi}_j \end{pmatrix} (\rho_{0,eq,j}, \phi_0; \rho_{k,eq,j}, \xi_k, \phi_s)$$

Determination of Voltage Modulation Index α_s

The gap voltage modulation index for the s^{th} cavity is given by (appendix D)

$$\alpha_s = \frac{|V_{g,s}|}{V_0} = G_0 Q_{T,s} \left(\frac{R}{Q} \right)_s \frac{\sqrt{\overline{C}_s^2 + \overline{D}_s^2}}{\sqrt{1 + 4Q_{T,s}^2 \delta_{T,s}^2}} \quad (18a)$$

and the RF gap voltage is given by

$$V_{g,s} = V_0 \alpha_s e^{j\theta_s} \quad (18b)$$

where

$$G_0 = \frac{I_0}{V_0}$$

$$Q_{T,s} = \frac{1}{\frac{1}{Q_{u,s}} + \frac{1}{Q_{ext,s}} + G_{b,s} \left(\frac{R}{Q} \right)_s} \quad (19)$$

$$\delta_{T,s} = \delta_{u,s} + \frac{B_{b,s}}{2} \left(\frac{R}{Q} \right)_s \quad (20)$$

$$\theta_s = -\arctan(2Q_{T,s}\delta_{T,s}) - \arctan \frac{\bar{D}_s}{\bar{C}_s} \quad (21)$$

and \bar{C}_s and \bar{D}_s are given by equations (16); $G_{b,s}$ and $B_{b,s}$ are given by equations (12) and (13); and $Q_{u,s}$, $Q_{ext,s}$, and $(R/Q)_s$ are design parameters.

COMPUTATION

Input Cavity, $s = 1$

Step 1: Perform the following computations:

(1) Compute the voltage modulation index α_1 by the relation

$$\begin{aligned} \alpha_1 &= \sqrt{\frac{2R_{sn,1}P_{in}}{V_0}} \\ &= \sqrt{\frac{2Q_{T,1}(R/Q)_1P_{in}}{V_0}} \end{aligned} \quad (22)$$

where P_{in} is the input power to the first cavity. Assuming that the input cavity presents a perfect match to the signal generator, we note that, since $Q_{load} = Q_{ext,1}$,

$$Q_{T,1} = \frac{1}{\frac{1}{Q_{u,1}} + G_{b,1} \left(\frac{R}{Q} \right)_1} \quad (22a)$$

If the beam loading effect is neglected, $Q_{T,1} = Q_{u,1}$.

(2) Compute the axial and radial beam coupling coefficients by using small-signal space-charge theory data given in the following:

$$M_{z,1} = \frac{\sin \theta_{g,1}}{\theta_{g,1}} \quad (23)$$

where $\theta_{g,1}$ is the gap half-transit angle defined by

$$\theta_{g,1} = \beta_e a \frac{\omega_1}{a}$$

$$M_{r,1} = \frac{\sqrt{I_0^2(\gamma b) - I_1^2(\gamma b)}}{I_0(\gamma a)} \quad (24)$$

in which I_0 and I_1 are the modified Bessel functions of the first kind, and

$$\gamma = \sqrt{\frac{\beta_e^2}{R_r} - k^2}$$

with

$$R_r = \frac{1}{\sqrt{1 - \left(\frac{u_0}{c}\right)^2}} \quad (25)$$

Step 2: Use the voltage modulation index α_1 obtained in step 1 to set up the velocity modulation of the beam, and by integrating the equations of motion (eqs. (1) and (2)) compute the bunched current at the second cavity gap. The initial conditions for the electrons are

$$\left. \begin{array}{l} z = z_0 = 0 \\ r = r_{0,eq,j} \end{array} \right\} \text{ for } t = t_0$$

or

$$\left. \begin{array}{l} \xi = 0 \\ \rho = \rho_{0,eq,j} \end{array} \right\} \text{ for } \theta = \theta_0$$

and

$$\left. \begin{array}{l} u_z = u_0 \\ u_r = 0 \end{array} \right\} \text{ for } t = t_0$$

or

$$\left. \begin{array}{l} \dot{\xi} = \frac{1}{\beta_e a} \\ \dot{\rho} = 0 \end{array} \right\} \text{ for } \theta = \theta_0$$

Second Cavity, $s = 2$

Step 1: Compute the fundamental beam current $I_{b,2}$ by using formulas derived from the linear space-charge wave theory. This is given by (ref. 2)

$$\frac{I_{b,2}}{I_0} = 2J_1 \left[\frac{\alpha_1 M_{z,1} M_{r,1}}{R_r(R_r + 1)} \cdot \frac{\omega}{\omega_q} \sin \left(\frac{\omega_q}{u_0} L_1 \right) \right] e^{j\Delta_{b,2}} \quad (26)$$

where

J_1 Bessel function of first kind

α_1 given by eq. (22)

$M_{z,1}$ given by eq. (23)

$M_{r,1}$ given by eq. (24)

R_r given by eq. (25)

$\Delta_{b,2} = -(\beta_e a)(L_1/a)$

L_1 length of drift tube between first and second cavities (see fig. 3)

ω_q reduced plasma frequency, $F\omega_p$

ω_p plasma frequency

F space charge reduction factor (determined from relation between $\beta_e b$ and a/b)

(For cylindrical beams in cylindrical tunnels, data on F can be found in ref. 2, fig. 3, p. 106, for instance.)

Step 2: Compute the induced current $I_{i,2}$ and induced voltage $V_{g,2}$ and hence obtain the gap voltage modulation index α_2 .

(1) The induced current (fundamental) is computed by small-signal theory formulas:

$$\frac{I_{i,2}}{I_0} = M_{z,2} M_{r,2} \left| \frac{I_{b,2}}{I_0} \right| e^{i\Delta_{i,2}} \quad (27)$$

where

$$M_{z,2} = \frac{\sin \theta_{g,2}}{\theta_{g,2}}$$

in which

$$\theta_{g,2} = \beta_e a \frac{L_2}{a}$$

By equation (25), $M_{r,2}$ can be obtained:

$$\Delta_{i,2} = \Delta_{b,2} = -\beta_e a \frac{L_2}{a}$$

(2) The fundamental induced gap voltage is given by equation (D6a) (appendix D); that is,

$$V_{g,2} = \frac{|I_{i,2}| Q_{T,2} \left(\frac{R}{Q}\right)_2 e^{j\theta_2}}{\sqrt{1 + 4Q_{T,2}^2 \delta_{T,2}^2}} \quad (28a)$$

where

$$\begin{aligned} \theta_2 &= \Delta_{i,2} - \arctan(2Q_{T,2} \delta_{T,2}) \\ &= \Delta_{b,2} - \arctan(2Q_{T,2} \delta_{T,2}) \end{aligned} \quad (28b)$$

$$Q_{T,2} = \frac{1}{\frac{1}{Q_{u,2}} + G_{b,2} \left(\frac{R}{Q}\right)_2} \quad (28c)$$

$$\delta_{T,2} = \delta_{u,2} + \frac{B_{b,2}}{2} \left(\frac{R}{Q}\right)_2 \quad (28d)$$

$$\begin{aligned} G_{b,2} &= \left| \frac{I_{b,2}}{I_0} \right| \frac{G_0}{\alpha_2} \cos[\arctan(2Q_{T,2} \delta_{T,2})] \\ &= \left| \frac{I_{b,2}}{I_0} \right| \frac{G_0}{\alpha_2} \frac{1}{\sqrt{1 + 4Q_{T,2}^2 \delta_{T,2}^2}} \end{aligned} \quad (28e)$$

$$\begin{aligned}
B_{b,2} &= \left| \frac{I_{b,2}}{I_0} \right| \frac{G_0}{\alpha_2} \sin[\arctan(2Q_{T,2}\delta_{T,2})] \\
&= \left| \frac{I_{b,2}}{I_0} \right| \frac{G_0}{\alpha_2} \frac{2Q_{T,2}\delta_{T,2}}{\sqrt{1 + 4Q_{T,2}^2\delta_{T,2}^2}}
\end{aligned} \tag{28f}$$

and

$$G_0 = \frac{I_0}{V_0}$$

Hence the gap voltage modulation index α_2 is

$$\alpha_2 = \frac{|V_{g,2}|}{V_0} = G_0 \left| \frac{I_{i,2}}{I_0} \right| \frac{Q_{T,2} \frac{R}{Q_2}}{\sqrt{1 + 4Q_{T,2}^2\delta_{T,2}^2}} \tag{29}$$

We notice that α_2 is a function of the beam loading parameters $G_{b,2}$ and $B_{b,2}$ which are, in turn, a function of the gap voltage. Hence, to compute α_2 , we require an iterative process. This is described in detail in the following:

(a) Initially, we find α_2 by computing $Q_{T,2}$ and $\delta_{T,2}$ by using data of $G_{b,2}$ and $B_{b,2}$ derived from small-signal theory:

$$\begin{aligned}
G_{b,2} &= -\frac{G_0}{2} \frac{\sin \theta_{g,2}}{\theta_{g,2}} \left(\frac{\sin \theta_{g,2}}{\theta_{g,2}} - \cos \theta_{g,2} \right) \\
&= -\frac{G_0}{2} M_{z,2} (M_{z,2} - \cos \theta_{g,2})
\end{aligned} \tag{30}$$

$$B_{b,2} = -\frac{G_0}{2} \left(\frac{\cos \theta_{g,2}}{\theta_{g,2}} \right) (M_{z,2} - \cos \theta_{g,2}) \tag{31}$$

The value obtained from equation (29) is given the name $\alpha_2(0)$, where the subscript (0) denotes the initial data for α_2 . In this manipulation, the values of $Q_{T,2}$ and $\delta_{T,2}$ obtained will be assigned the names $Q_{T,2}(0)$ and $\delta_{T,2}(0)$, respectively.

(b) In the next step, the values of $\alpha_2(0)$, $Q_{T,2}(0)$, and $\delta_{T,2}(0)$ are used to compute $G_{b,2}$ and $B_{b,2}$ from the large-signal equations (28e) and (28f), respectively. The data so obtained are given the name $G_{b,2}(1)$ and $B_{b,2}(1)$, where the subscript (1) denotes the first iteration data. These new data of $G_{b,2}(1)$ and $B_{b,2}(1)$ are used to compute $Q_{T,2}(1)$ and $\delta_{T,2}(1)$ from equations (28c) and (28d), respectively, and hence, to obtain a new gap modulation index, called $\alpha_2(1)$.

(c) After the first iteration process, we obtain an RF gap voltage $V_{g,2(1)}$ given by

$$V_{g,2(1)} = V_0 \alpha_{2(1)} e^{j\theta_{2(1)}} \quad (32a)$$

where

$$\theta_{2(1)} = \Delta_{b,2} - \arctan[2Q_{T,2(1)}\delta_{T,2(1)}] \quad (32b)$$

and this is to be compared with $V_{g,2(0)}$, which is defined in accordance with data obtained from the initial iteration process (a); that is,

$$V_{g,2(0)} = V_0 \alpha_{2(0)} e^{j\theta_{2(0)}} \quad (33a)$$

where

$$\theta_{2(0)} = \Delta_{b,2} - \arctan[2Q_{T,2(0)}\delta_{T,2(0)}] \quad (33b)$$

In order to compare two complex voltages, we must compare their magnitudes and phases separately as follows:

$$|\alpha_{2(1)} - \alpha_{2(0)}| \leq \epsilon_1$$

and

$$|\theta_{2(1)} - \theta_{2(0)}| \leq \epsilon_2$$

where ϵ_1 and ϵ_2 are two small specified values. If both of these inequality conditions are satisfied, we go to design step 3; otherwise we repeat procedures (a) and (b). This time the iteration process is initiated by using $\alpha_{2(1)}$ obtained in (b), and after the process has been repeated n times, finally the following inequality conditions are simultaneously satisfied:

$$|\alpha_{2(n)} - \alpha_{2(n-1)}| \leq \epsilon_1$$

and

$$|\theta_{2(n)} - \theta_{2(n-1)}| \leq \epsilon_2$$

Then, $\alpha_{2(n)}$ is the finalized value for α_2 . The word "simultaneously" requires an explanation. It simply means that both inequality conditions must be satisfied at the same time.

Step 3: The finalized value of $\alpha_2 (\equiv \alpha_2(n))$ described previously is used to set up the velocity modulation for gap 2. Thus the distance-step integration of the equations of motion is continued through the second drift-tube space L_2 until the third cavity gap is reached.

Third Cavity, $s = 3$

Step 1: Compute the Fourier coefficients \bar{A}_3, \bar{B}_3 , and \bar{C}_3, \bar{D}_3 of the fundamental beam current $I_{b,3}$ and the fundamental induced current $I_{i,3}$, respectively. The relevant equations to be used are (5) to (8) for $I_{b,3}$ and (15) to (17) for $I_{i,3}$. It is to be noted that the two velocity components, v_j and ξ_j , and the phase factors, ϕ_j and ϕ_m , are determined by the distance-step integration of the equations of motion initiated in step 3 of the last section.

Step 2: The Fourier coefficients \bar{A}_3, \bar{B}_3 and \bar{C}_3, \bar{D}_3 , obtained in step 1 are used to compute the gap voltage modulation index α_3 by using equation (18a). However, we note that α_3 , like α_2 , is a function of the beam loading parameters $G_{b,3}$ and $B_{b,3}$, which are, in turn, a function of the RF gap voltage $V_{g,3}$. Therefore α_3 can only be determined by means of an iterative process very similar to that described in the last section. Initially, the small-signal beam loading parameters, given by equations (30) and (31), are used to compute $Q_{T,3}(0)$ and $\delta_{T,3}(0)$ by using equations (19) and (20), where $Q_{ext,3} = \infty$ and $\delta_{u,3}$ is a design parameter. It is to be noted that, when equations (30) and (31) are used to compute $G_{b,3}(0)$ and $B_{b,3}(0)$, the gap transit angle θ_g should be computed by using the half-gap length ℓ_3 . In the next step, the values of $\alpha_3(0)$, $Q_{T,3}(0)$, and $\delta_{T,3}(0)$ obtained above together with the four Fourier coefficients obtained in step 1 are used to compute the beam loading parameters $G_{b,3}(1)$ and $B_{b,3}(1)$, by using equations (12) and (13) in this instance; $\alpha_3(1)$ is computed from equations (18) to (20). The iteration process described in the last section is followed through until a finalized value $\alpha_3(n)$ is obtained.

Step 3: Here, again, the finalized $\alpha_3 (\equiv \alpha_3(n))$ value is used to set up the velocity modulation for gap 3, and the distance-step integration of the equations of motion is continued through the third drift-tube space L_3 until the fourth cavity gap is reached.

Fourth Cavity, $s = 4$

Computations needed to design the fourth cavity follow exactly the same procedures described in the last section; however, great care must be exercised in choosing the appropriate design parameters for the various formulas. For instance, in computing the small-signal theory beam loading in the initial iteration process, ℓ_s should be used to compute the half-gap transit angle θ_g , etc.

The design of the fifth and sixth (if any) cavities follows in like manner.

Output Cavity

Step 1: Set the index s in various formulas in cavity 2 to its appropriate value; that is, for a five-cavity klystron, set s equal to 5.

Step 2: Compute the RF gap voltage $V_{g,s}$ from equation (18b), where the voltage modulation index for the output cavity α_s is obtained from an iterative process described in the sections Third Cavity, $s = 3$ and Fourth Cavity, $s = 4$. However, since the output cavity is coupled to an external matched load, some appropriate value (a design value) must be assigned to $Q_{ext,s}$ when computing $Q_{T,s}$ from equation (19). Moreover, since the output cavity is tuned to the input driving frequency, $\delta_{u,s}$ can be set equal to zero when computing $\delta_{T,s}$ from equation (20).

Step 3: The following additional computations are needed to complete the design of the output cavity:

(1) The fundamental conversion beam power, that is, the fundamental power taken from the beam by the output cavity, is given by

$$P_{conv} = \left(\frac{1}{2}\right) \text{Re } I_{ind,s} V_{g,out}^*$$

$$= \frac{Q_{T,s} \left(\frac{R}{Q}\right)_s (\bar{C}_s^2 + \bar{D}_s^2)}{2(1 + 4Q_{T,s}^2 \delta_{T,s}^2)} \cos[\arctan(2Q_{T,s} \delta_{T,s})]$$

This is maximum when $\cos[\arctan(2Q_{T,s} \delta_{T,s})]$ is equal unity, that is, when the following condition is satisfied:

$$\arctan(2Q_{T,s} \delta_{T,s}) = 2\pi k \quad \text{for } k = 0, 1, 2, \dots$$

(2) The conversion efficiency η_{conv} , or the electronic efficiency η_e , is given by

$$\eta_{conv} = \eta_e = \frac{P_{conv}}{I_0 V_0}$$

(3) The actual power delivered to the external matched load G_L is given by

$$P_{out} = \left(\frac{1}{2}\right) \text{Re } V_{g,s} I_{load}^*$$

$$= \left(\frac{1}{2}\right) G_L |V_{g,s}|^2$$

$$= \frac{V_0^2 \alpha_s^2}{2 \left(\frac{R}{Q}\right)_s Q_{ext,s}}$$

(4) The power gain of the klystron is defined by

$$\text{power gain} = \frac{P_{\text{out}}}{P_{\text{in}}}$$

(5) If $P_{\text{loss},s}$ is the heat dissipated in the output cavity wall, the output circuit efficiency is given by

$$\eta_{\text{cct}} = 1 - \frac{\text{power dissipated in cavity}}{\text{power supplied by beam}}$$

where power dissipated in the cavity is computed by

$$P_{\text{loss},s} = \frac{|V_{g,s}|^2}{2R_{\text{sh},s}} = P_{\text{out}} \frac{Q_{\text{ext},s}}{Q_{u,s}}$$

and $R_{\text{sh},s}$ is the shunt resistance due to wall and output coupling losses alone.

(6) If P_{col} is the power recovered in the depressed collector,

$$\eta_{\text{net}} = \frac{P_{\text{out}}}{\text{beam power} - P_{\text{col}}} = \frac{P_{\text{out}}}{I_0 V_0 - P_{\text{col}}}$$

APPENDIX A

DERIVATION OF EQUATIONS FOR CALCULATION OF $B_r(r,z)$ AND $B_z(r,z)$ OF DIRECT-CURRENT MAGNETIC FIELD

With reference to figure 2, we note that the vector potential $A(r,z)$ due to a single-layer close-wound solenoid of radius a_i and length L_{sc} is given by (ref. 3)

$$A_\theta(r,z) = C \int_0^\infty K_1(\lambda a_i) I_1(\lambda r) \cos \lambda z \sin\left(\frac{L_{sc}}{2}\right) \lambda \frac{d\lambda}{\lambda}$$

where I_1 and K_1 are modified Bessel functions of the first and second kind, respectively. The required magnetic field \vec{B} is obtained by taking curl of \vec{A} to obtain

$$\vec{B}(r,z) = \nabla \times \vec{A} = \hat{a}_r \left[-\frac{1}{r} \frac{\partial}{\partial z} (r A_\theta) \right] + \hat{a}_z \left[\frac{1}{r} \frac{\partial}{\partial r} (r A_\theta) \right] \quad (A1)$$

This gives

$$\begin{aligned} B_r(r,z) &= -\frac{\partial A_\theta}{\partial z} \\ &= C \int_0^\infty K_1(\lambda a_i) I_1(\lambda r) \sin \lambda z \sin\left(\frac{L_{sc}}{2}\right) \lambda d\lambda \end{aligned} \quad (A2)$$

and

$$\begin{aligned} B_z(r,z) &= -\frac{A_\theta}{r} + \frac{\partial A_\theta}{\partial r} \\ &= C \int_0^\infty K_1(\lambda a_i) I_0(\lambda r) \cos \lambda z \sin\left(\frac{L_{sc}}{2}\right) \lambda d\lambda \end{aligned} \quad (A3)$$

In order to evaluate the constant C , we require that

$$B_z(0,0) = B_0 \quad \text{for } r = 0 \quad \text{and } z = 0$$

where B_0 is the dc magnetic field along the z -axis, a design parameter. Thus, by letting $r = 0$ and $z = 0$, we have from equation (A3)

$$C = \frac{B_0}{\int_0^{\infty} K_1(\lambda a_i) \sin\left(\frac{L_{sc}}{2}\right) \lambda d\lambda} \quad (A4)$$

When the value of C is substituted into equations (A2) and (A3), we get

$$B_\rho(\rho, \xi) = \frac{B_0 \int_0^{\infty} K_1(\lambda a_i) I_1(\lambda \rho) \sin(\lambda \xi) \sin\left(\frac{L_{sc}}{2}\right) \lambda d\lambda}{\int_0^{\infty} K_1(\lambda a_i) \sin\left(\frac{L_{sc}}{2}\right) \lambda d\lambda} \quad (A5)$$

and

$$B_\xi(\rho, \xi) = \frac{B_0 \int_0^{\infty} K_1(\lambda a_i) I_0(\lambda \rho) \sin(\lambda \xi) \sin\left(\frac{L_{sc}}{2}\right) \lambda d\lambda}{\int_0^{\infty} K_1(\lambda a_i) \sin\left(\frac{L_{sc}}{2}\right) \lambda d\lambda} \quad (A6)$$

Equations (A5) and (A6) give us the radial and axial components of the dc magnetic field due to a close-wound single-layer solenoid. If the solenoid consists of N layers, the total magnetic field generated by this electro-magnet is obtained by summing all contributions of the N layers; that is,

$$B_\rho(\rho, \xi) = \sum_{i=1}^N B_0 \frac{\int_0^{\infty} K_1(\lambda a_i) I_1(\lambda \rho) \sin(\lambda \xi) \sin\left(\frac{L_{sc}}{2}\right) \lambda d\lambda}{\int_0^{\infty} K_1(\lambda a_i) \sin\left(\frac{L_{sc}}{2}\right) \lambda d\lambda} \quad (A7)$$

$$B_\xi(\rho, \xi) = \sum_{i=1}^N B_0 \frac{\int_0^{\infty} K_1(\lambda a_i) I_0(\lambda \rho) \sin(\lambda \xi) \sin\left(\frac{L_{sc}}{2}\right) \lambda d\lambda}{\int_0^{\infty} K_1(\lambda a_i) \sin\left(\frac{L_{sc}}{2}\right) \lambda d\lambda} \quad (A8)$$

where I_0 is the modified Bessel function of the first kind of the zero order, I_1 and K_1 are the modified Bessel function of the first and second kind, respectively, of the first order, and a_i is the radius of the i^{th} layer of the solenoid, with $i = 1, 2, \dots, N$.

APPENDIX B

DERIVATION OF EQUATIONS FOR CALCULATION OF BUNCHED CURRENT AND BEAM LOADING

The computation of the bunched current is based on the charge conservation principle. If the beam is divided into a number of disks of electrons and each disk is further divided into elementary charge rings (figs. 6 and 7), an elementary j^{th} ring $\pi(r_{0,0}^2 - r_{i,0}^2)\Delta z_0$ containing a charge Δq_0 at time t_0 at a later time t becomes Δq in an element of the charge ring $\Delta S \Delta z$. Thus, by the charge conservation principle, we obtain

$$\Delta q_0(r_0, z_0, t_0) = \Delta q(r, z, t)$$

or, more precisely,

$$\rho_0 \left(r_{0,0}^2 - r_{i,0}^2 \right)_j \Delta z_0 = \rho_j(r, z, t) \Delta S_j \Delta z \quad (\text{B1})$$

Since the rings are deformed and are permitted to change their axial and radial dimensions as well as their shape according to the total force acting on them, the right side of (B1) is employed to account for this fact; ΔS_j is the surface element of the j^{th} ring at time t . Equation (B1) can be written as

$$\begin{aligned} \rho_j(r, z, t) &= \rho_0(r_0, z_0, t_0) \frac{\pi \left(r_{0,0}^2 - r_{i,0}^2 \right)_j \frac{\Delta z_0}{\Delta z}}{\Delta S_j} \\ &= -J_{z0}(r_0, z_0, t_0) \frac{\pi \left(r_{0,0}^2 - r_{i,0}^2 \right)_j \frac{\Delta \phi_0}{\Delta \phi}}{u_z(r, z, t) \Delta S_j} \quad (\text{B2}) \end{aligned}$$

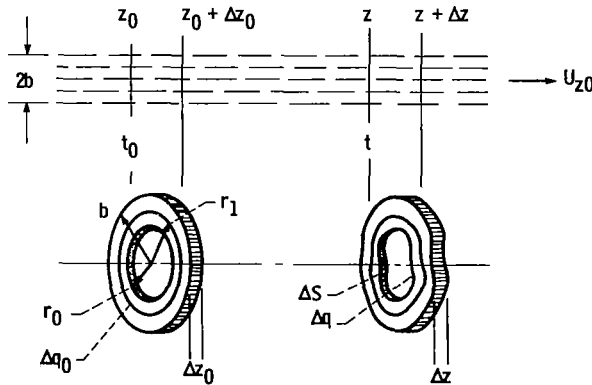


Figure 7. - Computation of charge conservation in deformed disks (rings).

where $\Delta z = u_z \Delta t$, $\Delta \phi = w \Delta t$, and $\Delta J_{z0} = -\rho_0 u_{z0}$. The density of the current carried by the charge element Δq_j at time t and some distance z from z_0 is given by

$$\begin{aligned}\vec{\Delta J}_j(r, z, t) &= \rho_j(r, z, t) \vec{u}_j(r, z, t) \\ &= \rho_j(r, z, t) u_z(r, z, t) \hat{a}_z + \rho_j(r, z, t) u_r(r, z, t) \hat{a}_r\end{aligned}$$

and the axial and radial components of the current density are given by

$$\begin{aligned}\Delta J_{zj}(r, z, t) &= \rho_j(r, z, t) u_{zj}(r, z, t) \\ &= -J_{z0}(r_0, z_0, t_0) \frac{\pi(r_{0,0}^2 - r_{i,0}^2)_j}{\Delta S_j} \frac{\Delta \phi_0}{\Delta \phi}\end{aligned}\quad (B3)$$

and

$$\Delta J_{rj}(r, z, t) = -J_{z0}(r_0, z_0, t_0) \frac{\pi(r_{0,0}^2 - r_{i,0}^2)_j}{\Delta S_j} \frac{u_{rj}(r, z, t)}{u_{zj}(r, z, t)} \frac{\Delta \phi_0}{\Delta \phi}\quad (B4)$$

respectively.

Assuming that there is no net current flow in the radial direction, we obtain the total current passing through a given plane perpendicular to the beam at an arbitrary distance z and the time t by summing all contributions from the charge elements that pass through this plane simultaneously at the time t . Hence

$$\begin{aligned}i_b(z_s, t_s) &= \sum_{j=1}^{j=NR} \Delta J_{z,j}(r, z_s, t_s) \Delta S_j \\ &= -\pi J_{z0}(r_0, z_0, t_0) \sum_{j=1}^{j=NR} \delta_{z,z_s} \left(r_{0,0}^2 - r_{i,0}^2 \right)_j \frac{\Delta \phi_0(r_0, z_0, t_0)}{\Delta \phi(r_0, t_0; z_s, t_s)}\end{aligned}\quad (B5)$$

where δ_{z,z_s} is the Kronecker delta notation defined by

$$\delta_{z,z_s} = 1 \quad \text{for } z = z_s$$

$$\delta_{z,z_s} = 0 \quad \text{for } z \neq z_s$$

and s is designated for the number of the cavity gap concerned. The summation process requires further explanation. Since in a high-density modulated electron beam each disk of electrons is deformed and distorted in shape, only a portion of the charge may cross a given cross-sectional plane at a given time; and at a given time, charges belonging to different disks may cross a given cross-sectional plane simultaneously. Only the ring charges whose arrival time at $z = z_s$ coincides will contribute to the bunched beam current.

In the next step, we expand the bunched current, equation (B5), in terms of Fourier series as follows:

$$i_b(z_s, t_s) = A_0 + \sum_{n=1}^{\infty} (A_n \cos n\phi + B_n \sin n\phi)$$

where

$$A_0 = \frac{1}{2\pi} \int_0^{2\pi} i_b(z_s, t_s) d\phi$$

This can be evaluated by using equation (B5) for $i_b(z_s, t_s)$ to obtain

$$A_0 = \left(\frac{1}{2}\right) J_{z0}(r_0, z_0, t_0) \int_0^{2\pi} \sum_{j=1}^{NR} \delta_{z,z_s} (r_{0,0}^2 - r_{i,0}^2)_j d\phi_0(r_0, z_0, t_0) \quad (B6)$$

and in like manner,

$$\begin{aligned} \begin{pmatrix} A_n \\ B_n \end{pmatrix} &= \frac{1}{\pi} \int_0^{2\pi} i_b(z_s, t_s) \begin{pmatrix} \cos n\phi \\ \sin n\phi \end{pmatrix} d\phi \\ &= -J_{z0}(r_0, z_0, t_0) \int_0^{2\pi} \sum_{j=1}^{NR} \delta_{z,z_s} (r_{0,0}^2 - r_{i,0}^2)_j \begin{pmatrix} \cos n\phi \\ \sin n\phi \end{pmatrix} d\phi_0(r_0, z_0, t_0) \end{aligned} \quad (B7)$$

Further evaluation of the coefficients A_0 , A_n , and B_n requires some thought. Let us consider the simpler case of the evaluation of A_0 first.

With reference to figure 6, we see that since by our choice each charge disk which enters the input cavity gap at equal time intervals is unmodulated, all the rings in a given disk will enter the input cavity gap simultaneously at a given time. Thus, if we use a double subscript to identify each of the NR charge rings instead of using a single index j , we can write equation (B6) as follows:

$$A_0 = -\left(\frac{1}{2}\right) J_{z0}(r_0, z_0, t_0) \sum_{\text{all } \Delta\phi_0} \sum_{n=1}^N \sum_{r=1}^R (r_{0,0,r}^2 - r_{i,0,r}^2)_n \Delta\phi_0$$

where the subscript r designates the ring of the disk, and the subscript n designates the disk number. With this new convention, we can represent $\Delta\phi_0$ by $2\pi/N$; hence

$$A_0 = -\left(\frac{1}{2}\right) J_{z0}\left(\frac{2\pi}{N}\right) \sum_{n=1}^N \sum_{r=1}^R (r_{0,0,r}^2 - r_{i,0,r}^2)_n$$

$$A_0 = -\frac{1}{N} \pi J_{z0}(r_0, z_0, t_0) \sum_{n=1}^N b_n^2$$

$$= -\frac{1}{N} \pi J_{z0}(r_0, z_0, t_0) (Nb^2) = -I_0 \quad (\text{B8})$$

where

$$\sum_{r=1}^R (r_{0,0,r}^2 - r_{i,0,r}^2)$$

is obviously the square of the beam radius b . This is the correct result for the coefficient A_0 . The evaluation of the coefficients A_n and B_n is not as simple since we are dealing with multiple value functions in the bunched beam. In this case, a single index representation may be least confusing. Thus, we shall represent $\Delta\phi_0$ by $(2\pi/NR)$. Using this convention, we may write equation (B7) as

$$\begin{pmatrix} A_n \\ B_n \end{pmatrix} = -\frac{2\pi}{NR} J_{z0}(r_0, z_0, t_0) \sum_{j=1}^{NR} (\delta_{z,z_s} r_{0,0}^2 - r_{i,0}^2)_j \begin{pmatrix} \cos n\phi_j \\ \sin n\phi_j \end{pmatrix} \quad (\text{B9})$$

where $\phi_j \equiv \phi_j(r_0, t_0; r, z_s, t_s)$ is a function of the radial position of the charge ring on crossing the constant z_s plane at time t_s , and hence,

it is to be determined by its radial position at the entrance r_0 and its entering time t_0 . In computer programming, it is more convenient to identify an individual ring by its equivalent charge center r_{eq} or r_e instead of its two radii, the outer radius r_0 and the inner radius r_i . Using this convention, we write equation (B9) as

$$\begin{pmatrix} A_n \\ B_n \end{pmatrix} = -\frac{2I_0}{b^2NR} \sum_{j=1}^{NR} \delta_{z,z_s} (r_{0,eq,j}^2) \begin{pmatrix} \cos n\phi_j(r_0,t_0;r,z_s,t_s) \\ \sin n\phi_j(r_0,t_0;r,z_s,t_s) \end{pmatrix} \quad (B10a)$$

where $I_0 = \pi b^2 J_{z0}$ is the dc beam current. In the expression for the equivalent charge center $r_{0,eq,j}$, the subscript 0 is referred to the unmodulated beam at the entrance to the input cavity gap. It is to be noted that, if each ring of the disks is divided into R rings, then, in accordance with the double index notation described previously, we have the following relation:

$$r_{0,eq,r}|_{n=1} = r_{0,eq,r}|_{n=2} = \dots = r_{0,eq,r}|_{n=N}$$

for $r = 1, 2, \dots, R$.

The equivalent charge centers for the case of $R = 3$ are computed by the following formulas as shown in figure 5:

$$\left. \begin{aligned} r_{0,1} &= \frac{bR}{\sqrt{3}} & r_{0,2} &= \frac{bR}{\sqrt{\frac{2}{3}}} & r_{0,3} &= bR \\ r_{0,eq,1} &= \frac{bR}{\sqrt{6}} & r_{0,eq,2} &= \frac{bR}{\sqrt{2}} & r_{0,eq,3} &= \frac{bR}{\sqrt{\frac{5}{6}}} \end{aligned} \right\} \quad (B10b)$$

In dealing with the beam loading problems, we require a complex expression for the beam current, and furthermore, our main concern is the fundamental beam current. Thus, by letting $n = 1$ in the Fourier series expansion formula, we obtain

$$\begin{aligned} i_b(z_s, t_s) &= A_0 + A_1 \cos \phi + B_1 \sin \phi \\ &= A_0 + \left(A_1^2 + B_1^2 \right)^{1/2} \cos(\phi - \Delta_b) \end{aligned} \quad (B11a)$$

with

$$\Delta_b = \arctan \left(\frac{B_1}{A_1} \right)$$

and the fundamental beam current $i_{b1}(z_s, t_s)$ given by

$$\begin{aligned} i_{b1}(z_s, t_s) &= (A_1^2 + B_1^2)^{1/2} \cos(\phi - \Delta_b) \\ &= \text{Re } \tilde{I}_{b1} \exp(j\phi) \end{aligned} \quad (\text{B11b})$$

where

$$\tilde{I}_{b1} = \sqrt{A_1^2 + B_1^2} \exp(-j\Delta_b) \quad (\text{B11c})$$

is the required complex beam current expression.

Finally it is convenient to normalize the complex beam current to the dc beam current I_0 . When this is done, we have the normalized beam current in complex form:

$$\tilde{\tilde{I}}_{b1} \equiv \frac{\tilde{I}_{b1}}{I_0} = \sqrt{\bar{A}_1^2 + \bar{B}_1^2} e^{-j\Delta_b} \quad (\text{B12a})$$

where

$$\begin{pmatrix} \bar{A}_1 \\ \bar{B}_1 \end{pmatrix} = -\frac{2}{b^2 \text{NR}} \sum_{j=1}^{\text{NR}} \delta_{z, z_s} \left(r_{0, \text{eq}, j}^2 \right) \begin{pmatrix} \cos \phi_j(r_0, t_0; r, z_s, t_s) \\ \sin \phi_j(r_0, t_0; r, z_s, t_s) \end{pmatrix} \quad (\text{B12b})$$

and

$$\Delta_b = \arctan\left(\frac{\bar{B}_1}{\bar{A}_1}\right) \quad (\text{B12c})$$

With the beam current determined, the beam loading effect can now be determined by computing the beam admittance Y_b as follows:

$$Y_b = \frac{\tilde{I}_{b1}}{\tilde{V}_g} = \frac{G_0}{\alpha} \sqrt{\bar{A}_1^2 + \bar{B}_1^2} e^{-j(\theta + \Delta_b)} \quad (\text{B13})$$

where

- I_{b1} complex beam current given by eq. (B11c)
 \tilde{V}_g complex gap voltage given by eq. (D6a)
 G_0 dc beam conductance, I_0/V_0
 α gap voltage modulation index, $|\tilde{V}_g|/V_0$
 \bar{A}_1, \bar{B}_1 normalized Fourier coefficients, given by eq. (B12b)
 Δ_b phase factor of complex beam current, $\arctan(\bar{B}_1/\bar{A}_1)$, given by eq. (B12c)
 θ phase factor of induced gap voltage, $\arctan(\bar{D}_1/\bar{C}_1) - \arctan(2Q_T\delta_T)$, given by eq. (D6b)

Finally the beam conductance G_b and beam susceptance B_b can now be obtained by taking the real and imaginary part of Y_b to yield

$$G_b = \text{Re } Y_b = \left(\frac{G_0}{\alpha} \right) \sqrt{\bar{A}_1^2 + \bar{B}_1^2} \cos(\theta + \Delta_b) \quad (\text{B14})$$

and

$$B_b = \text{Im } Y_b = \left(\frac{G_0}{\alpha} \right) \sqrt{\bar{A}_1^2 + \bar{B}_1^2} \sin(-\theta - \Delta_b) \quad (\text{B15})$$

APPENDIX C

DERIVATION OF EQUATIONS FOR CALCULATION OF INDUCED CURRENT

The calculation of the induced current is based on the general formulation, equation (37), derived in a previous report (ref. 1). This is rewritten in the following manner:

$$i_{ind}(z,t) = \sum_{\text{all } j} \rho_j \vec{u}_j \cdot \frac{\vec{E}_{cct,j}}{V_{ind}} \Delta t_j \quad (C1)$$

where

$\rho_j(r,z,t)$ charge density of j^{th} charge element

$\vec{u}_j(r_0, z_0; r, z, t)$ vector velocity of j^{th} charge element, which is function of entrance variables r_0 and t_0 , as well as its position (r, z) inside interaction gap at time t

$\vec{E}_{cct,j}(r_0, t_0; r, z, t)$ electric field induced in cavity by motion of charge element $\Delta q_j (= \rho_j \Delta t_j)$ inside interaction region, which is defined (fig. 8) as linear (extended) gap distance from $z_s - (1 + 2a)$ to $z_s + (1 + 2a)$, where z_s is referred to midplane of cavity gap, s^{th} cavity

V_{ind} induced voltage across cavity gap

The induced voltage V_{ind} is related to the cavity induced electric field amplitude E_0 by the following relation (see eq. (13)) of refs. 4 and 5):

$$E_0 = \frac{H |V_{ind,s}|}{(2 \sinh H\ell)} \quad (C2)$$

where $|V_{ind,s}|$ is the induced gap voltage of the s^{th} cavity, and H is the field-shape parameter. For a uniform field, $H = 0$. By the charge conservation principle, we can relate the charge element Δq_j in any

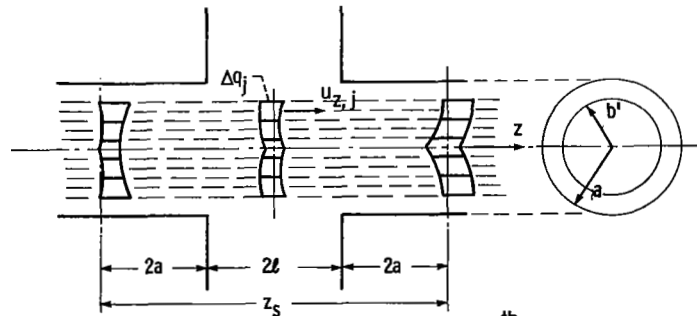


Figure 8. - Extended interaction gap configuration of the s^{th} cavity showing three deformed disk charges at various positions inside the gap at time $t = t_s$.

arbitrary interaction gap, the s th cavity gap, to the charge element $\Delta q_j (= \rho_0 \Delta t_j)$ at the entrance of the input cavity, where the beam is unmodulated and has a constant charge density ρ_0 . This, in turn, can be expressed as follows:

$$\Delta q_{0,j} = -\frac{Q}{NR} = -\frac{I_0}{NRf} = \Delta q_j$$

where I_0 is the dc beam current, f is the frequency of the klystron, and N and R are the total number of disks and rings used in the computer model. With this transformation, equation (C1) can be written as follows:

$$i_{ind}(z,t) = -\frac{I_0}{NRf} \sum_{j=1}^{NR} \vec{u}_j(r_0, t_0; r, z, t) \cdot \frac{\vec{E}_{cct,j}(r_0, t_0; r, z, t)}{V_{ind}}$$

where

$$z_s - (\ell + 2a) \leq z \leq z_s + (\ell + 2a)$$

This can be conveniently expressed by using Kronecker delta notation defined by

$$\delta_{z,z_k} = \begin{cases} 1 & \text{for } z = z_k \\ 0 & \text{for } z \neq z_k \end{cases}$$

where z_k is defined by

$$z_s - (\ell + 2a) \leq z_k \leq z_s + (\ell + 2a)$$

Thus

$$i_{ind}(t) = -\frac{I_0}{NRf} \sum_{\text{all } k} \delta_{z,z_k} \sum_{j=1}^{NR} \vec{u}_j(r, t; r, z, t) \cdot \frac{\vec{E}_{cct,j}(r, t; r, z, t)}{V_{ind}} \quad (C3)$$

Expressed in terms of its Fourier components, equation (C3) can be expanded as

$$i_{ind}(z_k, t) = C_0 + \sum_{n=1}^{\infty} (C_n \cos n\phi + D_n \sin n\phi) \quad (C4)$$

and, in particular, the fundamental component of the induced current, $i_{ind,1}$ is given by

$$\begin{aligned}
 i_{ind,1} &= \sqrt{C_1^2 + D_1^2} \cos(\phi - \Delta_i) \\
 &= \text{Re} \sqrt{C_1^2 + D_1^2} e^{-j\Delta_i} e^{j\phi} \\
 &= \text{Re} \tilde{I}_{ind,1} e^{j\phi}
 \end{aligned} \tag{C5}$$

where $\tilde{I}_{ind,1}$ is the complex expression for the induced current and is given by

$$\tilde{I}_{ind,1} = \sqrt{C_1^2 + D_1^2} e^{-j\Delta_i} \tag{C6a}$$

and

$$\Delta_i = \tan^{-1} \left(\frac{D_1}{C_1} \right) \tag{C6b}$$

in which C_1 and D_1 are the Fourier coefficients given by

$$\begin{aligned}
 \begin{pmatrix} C_1 \\ D_1 \end{pmatrix} &= \frac{1}{\pi} \int_0^{2\pi} i_{ind,1}(z_k, t) \begin{pmatrix} \cos \phi \\ \sin \phi \end{pmatrix} d\phi \\
 &= -\frac{I_0}{NRf} \sum_{\Delta\phi_m} \sum_{\text{all } k} \delta_{z, z_k} \sum_{j=1}^{NR} \left[\vec{u}_j(r_0, t_0; r, z_k t) \cdot \frac{\vec{E}_{cct, j}(r_0, t_0; r, z_k t)}{V_{ind}} \right] \\
 &\quad \times \begin{pmatrix} \cos \phi_m \\ \sin \phi_m \end{pmatrix} \Delta\phi_m
 \end{aligned}$$

$$= \frac{-I_0}{NRf} \left(\frac{2\pi}{M} \right) \sum_{m=1}^{M=36} \sum_{\text{all } z_k} \delta_{z,z_k} \sum_{j=1}^{NR} \left[\vec{u}_j(r_0, t_0; r, z_k t) \cdot \frac{\vec{E}_{cct,j}(r_0, t_0; r, z_k t)}{V_{ind}} \right] \times \begin{pmatrix} \cos \phi_m \\ \sin \phi_m \end{pmatrix} \quad (C6c)$$

In this equation, $\Delta\phi_m$ has been replaced by $(2\pi/M)$ and M is taken to be 36. Usually the fundamental induced current is normalized in terms of the dc beam current I_0 : then

$$\bar{I}_{ind,1} = \frac{I_{ind,1}}{I_0} = \sqrt{\bar{C}_1^2 + \bar{D}_1^2} e^{-j\Delta_i} \quad (C7a)$$

where

$$\Delta_i = \tan^{-1} \left(\frac{\bar{D}_1}{\bar{C}_1} \right) \quad (C7b)$$

and

$$\bar{C}_1 = \frac{C_1}{I_0} \quad (C7c)$$

$$\bar{D}_1 = \frac{D_1}{I_0} \quad (C7d)$$

Finally the dot product inside the bracket can be expressed in terms of its two scalar components in the form

$$\vec{u} \cdot \frac{\vec{E}}{V} = u_r \frac{E_r}{V} + u_z \frac{E_z}{V}$$

Using equation (C2), we obtain

$$\vec{u}_j \cdot \frac{\vec{E}_{cct,j}}{V_{ind}} = \frac{Ha\omega}{2 \sinh(H\ell)} \left[\rho_j \begin{pmatrix} F_\rho \\ G_\rho \end{pmatrix} + \xi_j \begin{pmatrix} F_\xi \\ G_\xi \end{pmatrix} \right]$$

By substituting this relation into equation (C6c), we get

$$\begin{aligned}
 \begin{pmatrix} C_1 \\ D_1 \end{pmatrix} = & - \frac{2\pi I_0 Ha}{MNR \sinh\left(Ha \frac{\ell}{a}\right)} \sum_{m=1}^{M=36} \sum_{\text{all } k} \delta_{z, z_k} \sum_{j=1}^{NR=(32)(3)} \\
 & \left[\begin{pmatrix} F_\rho \\ G_\rho \end{pmatrix} \dot{\rho}_j(r, t; r, z_k, t) + \begin{pmatrix} F_\xi \\ G_\xi \end{pmatrix} \dot{\xi}_j(r_0, t_0; r, z_k, t) \right] \\
 & \times \begin{pmatrix} \cos \phi_m(r_0, t_0; r, z_k, t) \\ \sin \phi_m(r_0, t_0; r, z_k, t) \end{pmatrix} \quad (C8)
 \end{aligned}$$

where

$$\dot{\rho}_j = \frac{u_{r,j}}{a\omega}$$

and

$$\dot{\xi}_j = \frac{u_{z,j}}{a\omega}$$

are the normalized velocity components in the radial and axial directions, respectively. They are functions of both the entrance position and phase as well as the position at the interaction gap and the time.

APPENDIX D
DERIVATION OF EQUATIONS FOR DETERMINATION
OF VOLTAGE MODULATION INDEX α

With reference to figure 9 and reference 6, we see that the input admittance of an arbitrary cavity is given by

$$Y_{in} = G_L + G_C + G_b + j\omega C + \frac{1}{j\omega L} + jB_b \quad (D1)$$

where

L cavity equivalent inductance

C cavity equivalent capacitance

G_C cavity conductance representing losses in a cold cavity, $1/R_0$

G_L equivalent load conductance as seen by cavity output window (perfect matched condition assumed), $1/R_L$

Y_b beam admittance, $G_b + jB_b$

G_b beam conductance, $\text{Re } Y_b$

B_b beam susceptance, $\text{Im } Y_b$

If we designate $G_T = G_C + G_b + G_L$ as the total shunt conductance of the cavity, then, in the vicinity of resonance, when the cavity is tuned to the higher side of the resonant frequency f_0 , by replacing $\omega = \omega_0 + \Delta\omega$, we can write equation (D1) as follows:

$$Y_{in} = G_T + jB_b + j\omega_0 C + j\Delta\omega C - j\frac{1}{\omega_0 L} \left(1 + \frac{\Delta\omega}{\omega_0}\right)^{-1} \\ \doteq G_T + j\left(B_b + \frac{2}{\omega_0 L} \frac{\Delta\omega}{\omega_0}\right) \quad (D2a)$$

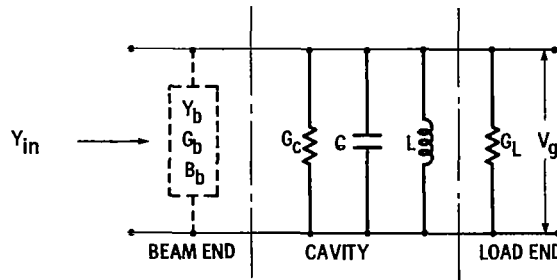


Figure 9. - Generalized cavity equivalent circuit.

To obtain equation (D2a), we used the following relations:

$$\frac{\Delta\omega}{\omega_0} \ll 1$$

$$j\omega_0 C + \frac{1}{j\omega_0 L} = 0$$

$$\omega_0^2 LC = 1$$

Furthermore, by denoting

$$\delta_u = \frac{\Delta\omega}{\omega_0}$$

and

$$\frac{R}{Q} = \sqrt{\frac{L}{C}}$$

we can write equation (D2a) as

$$Y_{in} = G_T \left[1 + j2Q_T \left(\delta_u + \frac{1}{2} B_b \frac{R}{Q} \right) \right] \quad (D2b)$$

where Q_T is the total or overall cavity Q defined by the following relation:

$$\frac{1}{Q_T} = \omega_0 L G_T = \frac{1}{Q_u} + \frac{1}{Q_e} + \frac{1}{Q_b} \quad (D3)$$

where

Q_u Q of the cavity that would result if the cavity were cold (i.e., in the absence of the beam) and no external load were coupled to it, $R_C/\omega_0 L$, with G_C or R_C representing losses in the cavity

Q_e Q that would result if the cavity were loss free and only loading by the external load were present, $R_L/\omega_0 L$

Q_b Q of the cavity due to beam loading alone, $1/\omega_0 L G_b = 1/G_b(R/Q)$

Next let us introduce the new parameter δ_T defined by

$$\delta_T = \delta_u + \left(\frac{1}{2} \right) B_b \left(\frac{R}{Q} \right) = \frac{(f_{drive} - f_{res})}{f_{res}} \quad (D4a)$$

where δ_u is the cavity frequency-detuning parameter in the absence of the beam, and $(1/2)B_b(R/Q)$ is the cavity frequency-detuning parameter due to the contribution of the beam susceptance B_b . In terms of this new frequency-detuning parameter δ_T , we write equation (D2b) as follows:

$$\begin{aligned} Y_{in}(\omega) &= G_T(1 + j2Q_T\delta_T) \\ &= G_T \sqrt{1 + (2Q_T\delta_T)^2} \arctan^{-1}(2Q_T\delta_T) \end{aligned} \quad (D4b)$$

With the input admittance of the cavity determined, the RF gap voltage can be found as follows:

$$\tilde{V}_g(\omega) = \frac{\tilde{I}_{ind,1}}{Y_{in}(\omega)} \quad (D5)$$

where $\tilde{I}_{ind,1}$ is the cavity induced current (fundamental) given by equation (C6a), and $Y_{in}(\omega)$ is the input admittance of the cavity given by equation (D4b). When these relations are substituted into equation (D5), we get the complex gap voltage

$$\tilde{V}_g = \frac{\sqrt{C_1^2 + D_1^2}}{\sqrt{1 + (2Q_T\delta_T)^2}} \frac{R}{Q} Q_T \arctan \theta \quad (D6a)$$

where we have replaced $R_T (= 1/G_T)$ by $(R/Q)Q_T$, and the phase angle of the voltage is given by

$$\theta = -\tan^{-1}\left(\frac{D_1}{C_1}\right) - \tan^{-1}(2Q_T\delta_T) \quad (D6b)$$

C_1 and D_1 are given by equation (C6c), and Q_T and δ_T are given by equation (D3) and (D4a), respectively.

Finally the voltage modulation index α can be obtained by taking the modulus of \tilde{V}_g divided by the dc beam voltage V_0 to yield

$$\alpha = \frac{|\tilde{V}_g|}{V_0} = G_0 Q_T \frac{R}{Q} \frac{\sqrt{C_1^2 + D_1^2}}{\sqrt{1 + (2Q_T\delta_T)^2}} \quad (D7)$$

where $G_0 = I_0/V_0$ is the dc beam conductance, and \bar{C}_1 and \bar{D}_1 are the normalized Fourier coefficients given by equation (C7).

REFERENCES

1. Kosmahl, Henry G.: Three-Dimensional Relativistic Field-Electron Interaction in a Multicavity High-Power Klystron. I - Basic Theory. NASA TP-1992, 1982.
2. Beck, A. H. W.: Space Charge Waves and Slow Electromagnetic Waves. Pergamon Press, 1958.
3. Smythe, William Ralph: Static and Dynamic Electricity. Second ed. McGraw-Hill Book Co., Inc., 1950, p. 267.
4. Kosmahl, Henry G.; and Branch, Garland M.: Generalized Representation of Electric Fields in Interaction Gaps of Klystrons and Traveling Wave Tubes. IEEE Trans. Electron Devices, vol. ED-20, no. 7, July 1973, pp. 621-629.
5. Kosmahl, Henry D.; and Albers, Lynn U.: Three-Dimensional Evaluation of Energy Extraction in Output Cavities of Klystron Amplifiers. IEEE Trans. Electron Devices, vol. ED-20, no. 10, Oct. 1973, pp. 883-890.
6. Lien, E.: High-Efficiency Klystron Amplifiers. 8th International Conference on Microwave and Optical Generation and Amplification, Amsterdam, The Netherlands, Sept. 1970, Kluwer (Deventer, Netherlands), 1971, pp. 11-21 to 11-27.

1. Report No. NASA TP-2008		2. Government Accession No.		3. Recipient's Catalog No.	
4. Title and Subtitle THREE-DIMENSIONAL RELATIVISTIC FIELD-ELECTRON INTERACTION IN A MULTICAVITY HIGH-POWER KLYSTRON II - WORKING EQUATIONS				5. Report Date April 1982	
				6. Performing Organization Code 506-61-22	
7. Author(s) Henry G. Kosmahl				8. Performing Organization Report No. E-1018	
				10. Work Unit No.	
9. Performing Organization Name and Address National Aeronautics and Space Administration Lewis Research Center Cleveland, Ohio 44135				11. Contract or Grant No.	
				13. Type of Report and Period Covered Technical Paper	
12. Sponsoring Agency Name and Address National Aeronautics and Space Administration Washington, D.C. 20546				14. Sponsoring Agency Code	
15. Supplementary Notes Material, not previously published, presented at the International Electrons Devices Meeting sponsored by the Institute of Electrical and Electronic Engineers, Washington, D.C., October 11, 1971, and the Solar Power Space System Workshop sponsored by NASA Lyndon B. Johnson Space Center, Houston, Texas, January 15-18, 1979.					
16. Abstract A computation package containing all equations and procedures needed in designing a high-power multicavity klystron amplifier has been developed. The rigorously derived three-dimensional relativistic axisymmetric equations of motion are used to compute the bunched current and the induced RF gap voltage for all interaction cavities except the input and second cavities, where the linear space-charge wave theory data are employed in order to reduce the computation time. Both distance-step and time-step integration methods are used to compute the Fourier coefficients of both the beam current and induced current.					
17. Key Words (Suggested by Author(s)) Equations for a three-dimensional relativistic multicavity klystron amplifier; Bunching and induced voltages			18. Distribution Statement Unclassified - unlimited STAR Category 33		
19. Security Classif. (of this report) Unclassified		20. Security Classif. (of this page) Unclassified		22. Price* A03	
				21. No. of Pages 42	